SCIENCE CHINA Materials

ARTICLES

mater.scichina.com link.springer.com

Published online 19 August 2015 | doi: 10.1007/s40843-015-0074-x
Sci China Mater 2015, 58: 603–610

Synthesis of high quality nitrogen-doped single-wall carbon nanotubes

Peng-Xiang Hou†, Man Song†, Jin-Cheng Li, Chang Liu*, Shi-Sheng Li and Hui-Ming Cheng

Nitrogen-doped single-wall carbon nanotubes (SWCNTs) with diameters in the range of 1.1–1.6 nm were synthesized on a large scale by floating catalyst chemical vapor deposition. Ferrocene, methane and melamine were respectively used as the catalyst precursor, carbon source and nitrogen source. The content of nitrogen introduced into the SWCNT lattice was characterized to be ~0.4 at.%. This resulted in a decreased mean diameter, narrower tube diameter distribution, and increased surface area of the SWCNTs. The temperatures at which the rate of weight loss reaches the maximum value for N-SWCNTs are ~785°C, similar to that of pure SWCNTs, indicative of their high-quality and good crystallinity. These N-SWCNTs exhibited a metallic behavior and desirable electrochemical oxygen reduction reaction activity.

INTRODUCTION

Single-wall carbon nanotubes (SWCNTs) are considered as an ideal building block of next-generation nanodevices due to their unique electronic, optical, optoelectronic, and mechanical properties [1,2]. SWCNTs can be either metallic or semiconducting depending on their chiral angle and diameters. Semiconducting SWCNTs (s-SWCNTs) can be used in field effect transistors (FETs) and optoelectronic devices as a channel material [3–7], while metallic SWCNTs (m-SWCNTs) are ideal interconnectors in integrated circuits and high-frequency devices [8–10]. However, real applications of m- and s-SWCNTs are hindered by the fact that SWCNT samples are usually a mixture of metallic and semiconducting types, which leads to very poor performance and non-uniformity of the fabricated devices. It is therefore very important to prepare SWCNTs of a single electrical type. In recent years, notable progress has been made in the selective growth of s-SWCNTs by *in situ* etching of m-SWCNTs, based on the principle that m-SWCNTs are usually chemically more active than s-SWCNTs [11–13]. However, the direct growth of m-SWCNTs seems to be more difficult [14–18].

Substitutional doping of heteroatoms in the SWCNT lattice has proven to be an efficient way of tuning the band-gap and workfunction [19], since it substantially modifies the atomic structures [20,21] and chemical reactivity [22], and consequently their range of possible applications is significantly broadened. In general, due to the small mismatch in atomic sizes, boron (B) and nitrogen (N) have been the most frequently used dopants of SWCNTs rather than sulphur, phosphorus, and silicon with an obvious size mismatch [23–26]. In particular, N-doping of SWCNTs has been extensively studied due to the simple and easy doping process. It has been shown that the introduction of N can greatly influence the growth of SWCNTs by changing chiral angles [27], decreasing diameters [28], and reducing growth rates [29,30]. Most previous studies intended to introduce a high-content of N into SWCNTs, so that the band gap of SWCNTs would be significantly changed. However, structural defects are then inevitably introduced into the SWCNTs, which results in the deterioration of their electrical/thermal conductivity and mechanical properties [31,32]. In this case, the overall effects of N-doping on the properties of SWCNTs turn out to be complex and unclear. Therefore, there is a great need to achieve band-gap tuning of SWCNTs by N-doping without adversely affecting their physical properties. A feasible way to retain the high crystallinity of tube walls, is to dope with only small amounts of N. Pint *et al.* [33] reported the synthesis of SWCNT arrays containing a limited amount of nitrogen, but the properties of the resulting materials were not investigated.

In this study, we prepared high-quality N-doped SWCNTs on a large scale by a floating catalytic chemical vapor deposition (FCCVD) method. Thermogravimetry-mass spectrometry measurements (TG-MS) and X-ray photoelectron spectroscopy (XPS) analysis confirmed that a very low content of nitrogen was doped into the tube lattices without significantly changing their crystallinity. Furthermore, the N-doping leads to a lower mean diameter, a narrower

Shenyang National Laboratory for Materials Science, Institute of Metal Research, Chinese Academy of Sciences, Shenyang 110016, China
† These authors contributed equally to this work.
* Corresponding author (email: cliu@imr.ac.cn)

diameter distribution, and an increased specific surface area. More importantly, the N-doped SWCNTs show metallic behavior and excellent electrocatalytic activity for the oxygen reduction reaction.

EXPERIMENTAL DETAILS

Synthesis of N-doped SWCNTs

The N-doped (denoted N-) SWCNTs were synthesized by a common FCCVD method [11,34] at 1100°C. Ferrocene, melamine, and sulfur powders with a weight ratio of 100:100:1 were pressed into a pellet, and then used as the catalyst precursor, nitrogen source, and growth promoter, respectively. A 500 sccm H_2 flow was introduced into a 25 mm-diameter quartz tube reactor placed in a horizontal tubular furnace. When the temperature of the reactor was increased to 1100°C, the ferrocene/melamine/sulfur pellet was pushed into the upstream of the reactor (where the temperature was ~125°C). These materials sublimed and were carried into the reaction zone by H_2 gas flow. At the same time, a flow of 4.5 sccm CH_4 was introduced into the reactor as the carbon source. The synthesis process lasted for 45 min. Finally, the reactor was naturally cooled to room temperature. Pure (denoted as P-) SWCNTs were also synthesized for comparison under identical conditions except that melamine was not added.

Purification of SWCNTs

The as-prepared SWCNTs were heat treated at 350°C in air for 2 h and then immersed in hydrochloric acid for 30 min at 80°C. The samples were then thoroughly washed using deionized water and further annealed at 400°C under an Ar flow for 1 h.

Characterization

The SWCNTs were characterized by scanning electron microscopy (SEM, Nova NanoSEM 430, 15 kV), transmission electron microscopy (TEM, JOEL 2010 operated in 200 kV), XPS (Escalab 250, Al Kα), Raman spectroscopy (Jobin Yvon HR800), and TG-MS (Netsch STA 449C, Jupiter +QMS 403C).

Construction of thin film field effect transistors (TFTs)

TFTs were fabricated using SWCNTs as the channel material. SWCNT thin films were collected using the method described in [11]. Briefly, a filter was installed and connected to the tail gas pipe of the SWCNT growth reactor. The as-synthesized SWCNTs were carried into this pipe by H_2 carrier gas and were collected by the filter. The collection is a gas phase process, so no solution or chemical was introduced. A Si wafer with pre-set Au electrodes was placed on the filter, and the SWCNTs were directly deposited as a channel material on the Si wafer.

Oxygen reduction reaction (ORR) measurements

Cyclic voltammetry (CV) measurements were performed using a program-controlled potentiostat (CHI 730 C) in a standard three-electrode cell. An SWCNT electrode was used as working electrode and a Pt wire served as counter electrode. For ORR measurements, an aqueous solution of KOH (0.1 M) was used as electrolyte, and an Ag/AgCl electrode (10% KNO_3 solution filled) as reference electrode. O_2 was used to purge the solution to obtain oxygen-saturated electrolyte solutions. Tests were performed at a scan rate of 100 mV s^{-1}. The SWCNTs were ultrasonically dispersed in an ethanol solution containing 0.05 wt.% Nafion to form a concentration of 1.0 mg mL^{-1} catalyst ink, then coated on the surface of a glassy carbon disk (5.0 mm diameter). The catalyst loading was 0.1 mg cm^{-2}. Measurements on a rotating disk electrode were carried out on a modulated speed rotator electrode rotator (Pine Instruments). For quantitative evaluation of the ORR electrocatalytic activity, rotating disk electrode (RDE) measurements were performed and analyzed using the Koutecky-Levich (K-L) equation.

RESULTS AND DISCUSSION

Structure of the N-SWCNTs

SEM images of the N- and P-SWCNTs after the simple purification process are shown in Fig. S1. Randomly entangled long SWCNTs were observed, and there is no obvious morphology difference between the two types. TEM observation of the purified N- and P-SWCNTs shows that both are composed of random SWCNT bundles (Figs 1a and S2a). The diameters of about 80 SWCNTs from each sample were measured under TEM, and the resultant histograms showing their diameter distributions are shown in Figs 1b and S2b. The N-doped SWCNTs have diameters mostly in the range of 1.0–1.6 nm, and centered at ~1.28 nm (Figs 1a and b), while the diameters of the P-SWCNTs are distributed in two regions centered at 1.38 nm and 1.86 nm (Fig. S2b). We note that SWCNTs with diameters larger than 2.0 nm can be occasionally observed in the P-SWCNTs but are rarely seen in the N-doped SWCNTs. Therefore, the diameters of the N-SWCNTs are smaller than those of the P-SWCNTs, and their diameter distribution is narrower.

The pore structures of the N- and P-SWCNTs were investigated by cryo-nitrogen adsorption measurements and the adsorption isotherms were analyzed using the density functional theory (DFT) equation. Prior to the measure-

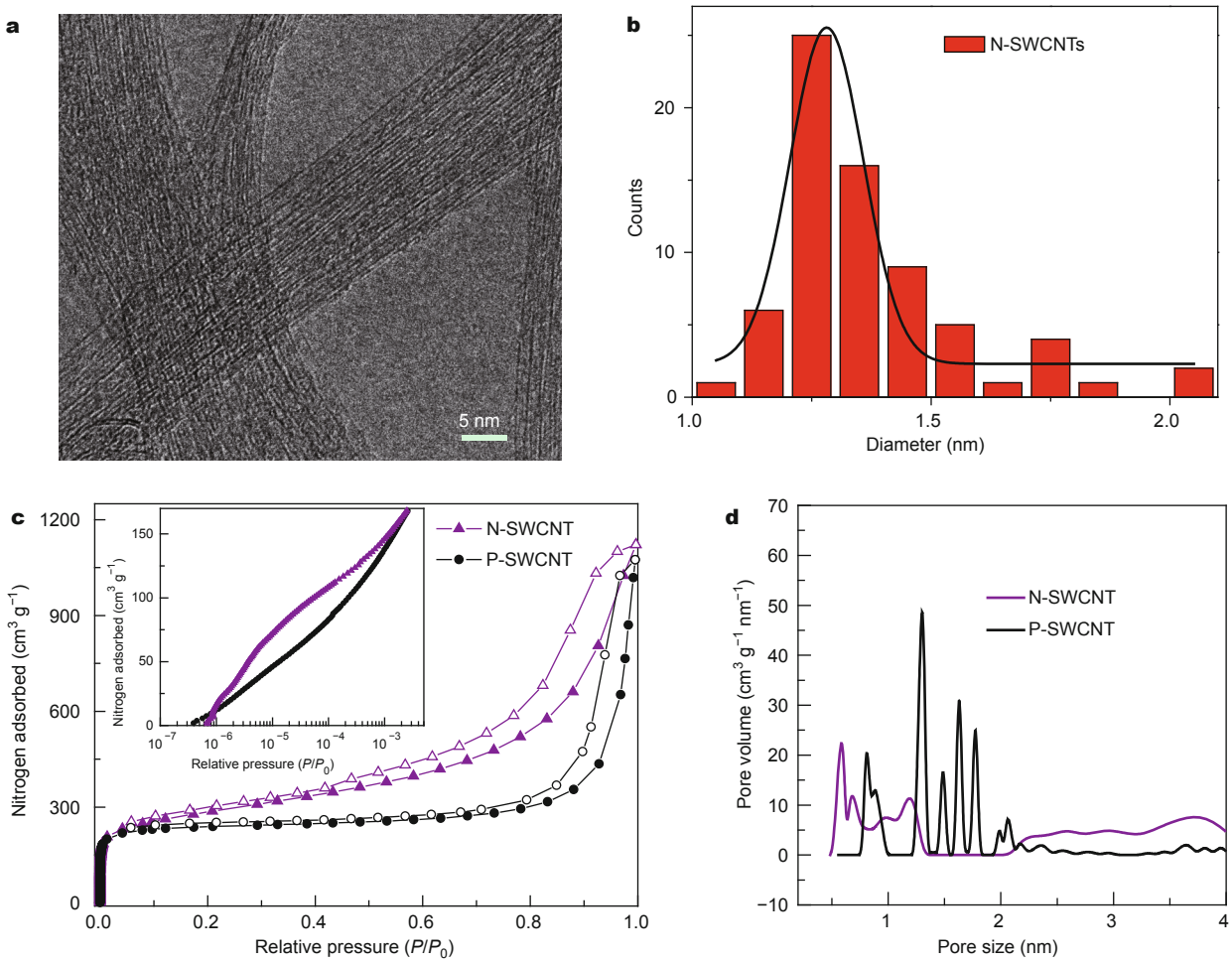

Figure 1 (a) Typical TEM image of the N-SWCNTs. (b) Histogram of the diameter distribution of N-SWCNTs based on TEM observations and measurements. The fitted mean diameter is 1.28 nm. (c) N_2 adsorption isotherms of the N- and P-SWCNTs, the inset shows logarithmic plots at extremely low pressure. (d) DFT pore size distributions of the N- and P-SWCNTs.

ments, the caps of the SWCNTs were opened by a controllable oxidation technique [35] to allow N_2 to access the CNT cores. The nitrogen adsorption isotherms of the P-SWCNTs and N-SWCNTs are shown in Fig. 1c and exhibit two common features: a drastic increase of adsorption near 0 relative pressure and a small hysteresis behavior between the adsorption/desorption loops. Logarithmic plots of the N_2 adsorption isotherms in the extremely low P/P_0 (10^{-7}–10^{-3}) region are given in the inset of Fig. 1c. Obviously, the amount adsorbed by the N-SWCNTs is much higher than that of the P-SWCNTs. The BET surface areas calculated from the adsorption isotherms are 910 and 590 $m^2\ g^{-1}$ for the N-SWCNTs and P-SWCNTs, respectively. To obtain more detailed information of their pore structures, pore size distribution (PSD) curves were obtained using the DFT equation (available in the ASAP2020 software) and are shown in Fig. 1d. It can be seen that the micropore sizes of the N-SWCNTs are narrowly distributed in the range of 0.6–1.3 nm, compared to the wider pore size distribution of the P-SWCNTs that ranges from 0.8 to 2.1 nm. Considering the C atom covalent diameter of 0.15 nm, the pore size distribution is consistent with the results of HRTEM observations for both the P- and N-SWCNTs [36–38]. These results confirm the previous reports that N-doping leads to a decreased mean tube diameter and a narrower diameter distribution [21,39].

To investigate the effect of nitrogen doping on the stability of SWCNTs, thermogravimetric analysis (TGA) of the N- and P-SWCNTs was performed under a mixed air (50 sccm) and nitrogen (50 sccm) flow, and the corresponding curves are shown in Figs 2a and S3a. It can be seen that major weight loss occurs in the temperature range of 600–

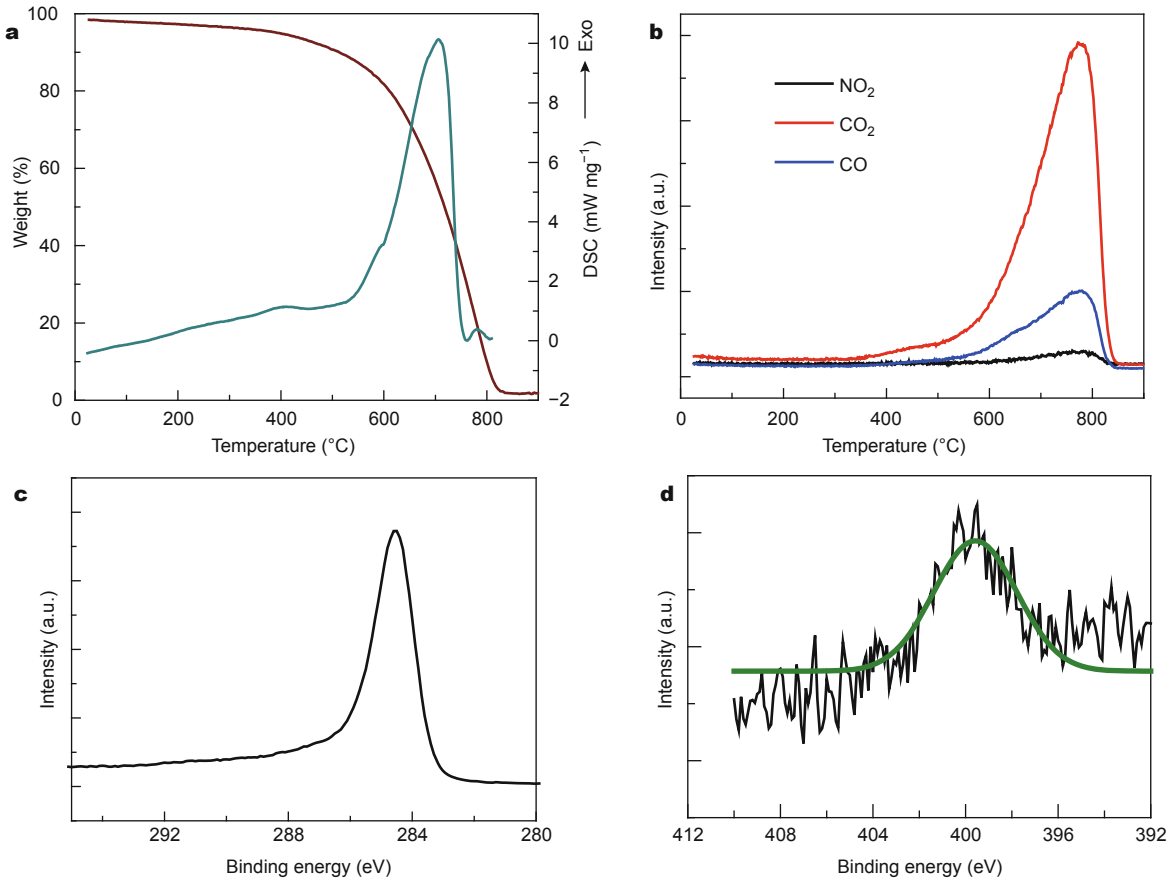

Figure 2 (a) TG/DSC curves of the N-SWCNTs. (b) TG-MS analysis of the N-SWCNTs. (c) and (d) C1s and N1s XPS spectra of the N-SWCNTs.

800°C for both samples. The temperatures at which the rate of weight loss reaches the maximum value for the P- and N-SWCNTs are ~800 and 785°C, respectively. Even though this temperature for N-SWCNTs is slightly lower than that for P-SWCNTs, if one takes account of the smaller diameter (larger curvature) of the N-SWCNTs, which leads to higher chemical reactivity [40], it appears that the crystallinity of the N-SWCNTs is not deteriorated by the N doping, which is consistent with the TEM observations.

Determination of N-doping

XPS, TG-MS [33,41] and laser Raman analysis were performed to characterize the N-SWCNTs. TG-MS analysis is able to differentiate whether the nitrogen atoms are doped into the carbon lattice or just adsorbed on the surface. As shown in Fig. 2b, an NO_2 signal was detected in the N-SWCNT sample, but not in the P-SWCNT sample. More importantly, CO and CO_2 signals started to appear at about 400°C, which corresponds to the decomposition temperature of carbons containing defects. The NO_2 signal was detected at about 600°C and the highest NO_2 release peak was at 785°C, similar to those of CO_2 and CO. This temperature is consistent with the temperature of the fastest oxidation of the N-SWCNTs (Fig. 2a). The NO_2 starts to be released at about 600°C, indicating that the nitrogen is not adsorbed on the tube walls or exist as functional groups at the tube surface. The simultaneous release of CO_2 and NO_2 further confirms that the N is doped into the sp^2 lattice of the SWCNTs.

In order to quantitatively determine the amount and type of N doping, XPS characterization of the P- and N-SWCNTs was performed. As shown in Fig. 2c, a main C1s peak appears at 284.5 eV for the N-SWCNTs, and there is no obvious difference from that of the P-SWCNTs (Fig. S3c). However, a small N1s peak was observed at 399.5 eV for the N-SWCNTs (Fig. 2d), corresponding to pyridinic nitrogen. The nitrogen content calculated from the area ratio of N1s to C1s signals corrected with standard XPS sensitivity factors was only 0.4 at.%. The above results indicate that a very low amount of N was doped in the lattice of the

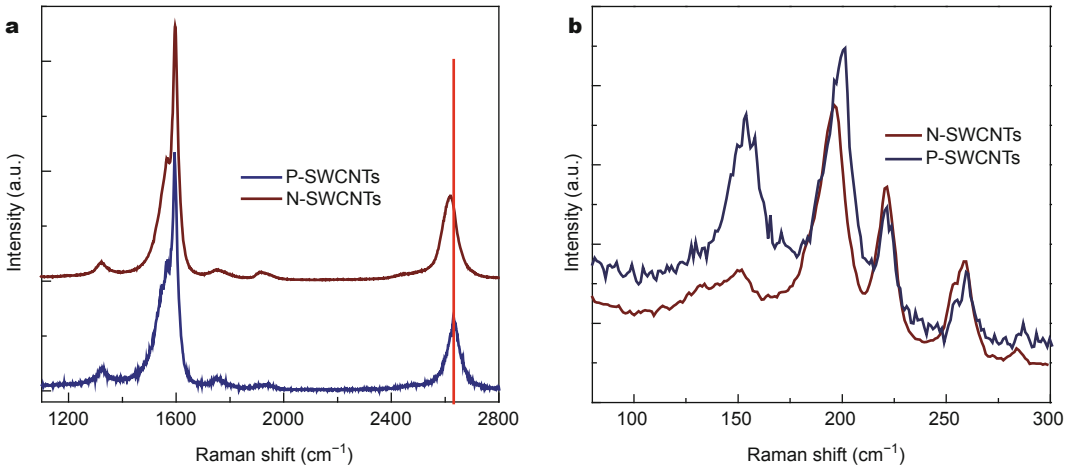

Figure 3 Laser Raman spectra of the N- and P-SWCNTs. (a) G and G' mode. (b) Radial breathing mode.

N-SWCNTs.

The G' band in the Raman spectrum of SWCNTs is highly sensitive to electronic interaction with charged species occupying SWCNT lattice sites [42,43]. Therefore, the G' band has been considered as a characteristic of substitutional doping in SWCNTs [23]. Previous reports have pointed out that the G' mode would make a red-shift and generate a $G'_{N\text{-}dope}$ peak at a lower frequency for nitrogen-doped nanotubes compared with their pristine counterparts [42]. Fig. 4a shows the Raman G' bands of the N- and P-SWCNTs excited by a 1.96 eV laser. It can be seen that the G' peak of the N-SWCNTs is down-shifted by about 9 cm^{-1} compared with that of the P-SWCNTs, which further confirms that nitrogen is doped into the N-SWCNT lattice. Fig. 4b shows typical radial breathing mode peaks of the N- and P-SWCNTs. The intensities of the low frequency peaks obviously decrease after nitrogen doping, which indicates that the number of large diameter nanotubes is lower in the N-SWCNTs, consistent with the TEM and cryo-nitrogen adsorption characterizations.

TFTs based on the N-doped SWCNTs

Terrones *et al.* [26] predicted theoretically that for N-doped s-SWCNTs, the electronic state created by nitrogen doping lies beneath the conduction bands and is occupied by an extra electron. The Fermi level is shifted close to the conduction bands, causing all semiconducting SWCNTs to be metallic. To test the metallicity of the as-grown N-SWCNTs, TFTs based on the N-SWCNTs were fabricated, and their properties were studied. Thin films comprised of low density SWCNT random networks were collected by directly depositing the N-SWCNTs grown by FCCVD on a silicon wafer with preset gold electrodes placed in the downstream of the reactor. Fig. 4a shows a diagram of these TFT de-

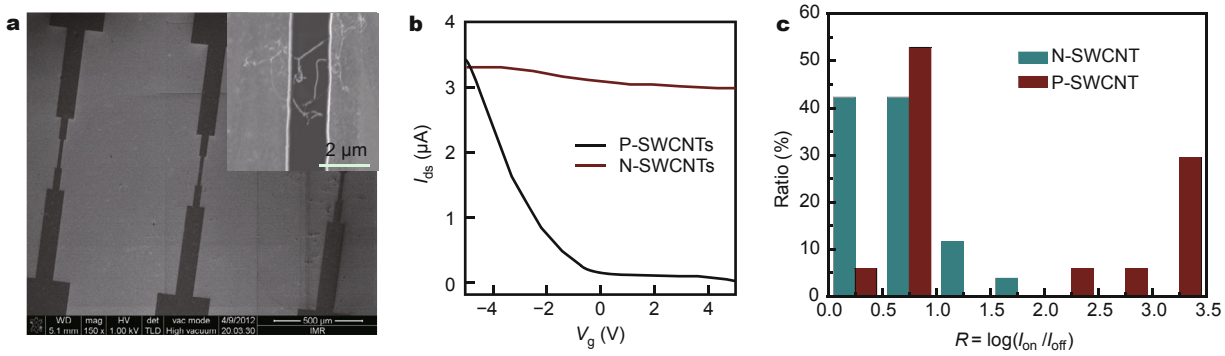

Figure 4 (a) SEM images of an N-SWCNT-based TFT. The width of the source and drain Au electrodes is 20 μm, and the channel length is 2 μm, constructed on a 100-nm thick SiO_2/Si substrate (inset: high magnification SEM image showing the channel structure of the TFT). (b) Typical transport characteristics and (c) statistical current on/off ratios of the TFTs fabricated using the N- and P-SWCNTs.

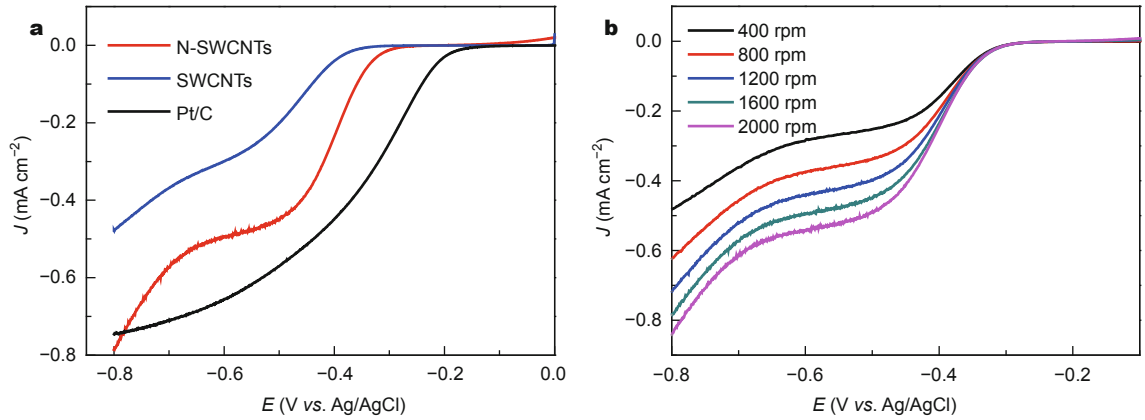

Figure 5 RDE voltammograms in an O_2-saturated 0.1 M KOH solution at room temperature (rotation speed 1600 rpm, sweep rate 100 mV s^{-1}) for the N-SWCNTs, P-SWCNTs and Pt/C. b) RDE voltammograms for ORR of the N-SWCNT electrode at various rotation speeds (sweep rate 100 mV s^{-1}).

vices. SEM observation (inset of Fig. 4a) shows that some sparsely distributed SWCNTs connect the source and drain electrodes. Fig. 4b shows typical I_{sd} – V_g curves of the P- and N-SWCNT-based TFTs.

In total, 50 TFTs based on N-doped SWCNTs were constructed, and measurements indicate that 43 of the 50 have current on/off ratios lower than 10, and the other 7 have values in the range of 10–100. In a parallel comparative experiment using P-SWCNTs, 29 of 50 have current on/off ratios larger than 10, and the other 21 have values larger than 100. Fig. 4c shows the histograms of the statistical results for the TFTs based on the N- and P-SWCNTs and these confirm that the N-SWCNTs exhibit metallic behavior, i.e. the content of metallic SWCNTs increases remarkably on N-doping as predicted.

Catalytic oxygen reduction property of the N-doped SWCNTs

N-doped CNTs have been reported to have high electrocatalytic activity for the ORR as a result of the increased surface chemical reactivity arising from the modification of surface properties due to the electronegativity of doped nitrogen [44]. In contrast, pure SWCNTs have a low surface energy arising from neutral C–C bonding. As described above, we prepared metallic N-SWCNTs with high surface area and small diameter, so their superior electrocatalytic activity should be expected. CV and RDE measurements were performed to investigate the ORR activity of the N-SWCNTs. For comparison, the P-SWCNTs and commercial 20 wt.% platinum on carbon black (Pt/C) were also measured under identical conditions. The results show that the values of the onset potentials of N-SWCNTs, P-SWCNTs and Pt/C were −203, −281 and −78 mV, respectively (Fig. 5a). Remarkably, the N-SWCNT electrode exhibits a more positive onset potential than the P-SWCNT electrode. The positive-shift of the onset potential and increased reduction current achieved by the N-SWCNT electrode indicates that N-SWCNTs have a much higher electrocatalytic activity toward ORR than the P-SWCNTs. Fig. 5b shows the RDE voltammograms of the N-SWCNT electrode at various rotation speeds. The kinetic parameters were analyzed with the K-L equations. Fig. S4a shows the corresponding K-L plots (J^{-1} *vs.* $\omega^{-1/2}$) and it can be seen that the data exhibit good linearity. The number of electrons transferred (n) was estimated to be 2.65 at potentials ranging from −0.4 to −0.7 V. Fig. S5 shows the RDE voltammograms for ORR of the P-SWCNT electrode. The number of electrons transferred was estimated to be 2.32 from the corresponding K-L plots (Fig. S4b), which indicates that the ORR process catalyzed by the SWCNTs is a two-electron pathway. We attribute this better ORR performance of the N-SWCNT catalyst to its unique structure with a high surface area, pyridinic nitrogen doping, and high quality of carbon lattice, which simultaneously produces a high-density of active sites, and good electrical conductivity.

CONCLUSIONS

N-doped SWCNTs with low nitrogen content were synthesized on a large-scale by a FCCVD method. The tubes have a narrow distribution of diameters in the range of 1.1–1.6 nm and a high specific surface area of 910 $m^2 g^{-1}$. XPS and TG-MS measurements show that the N occupies lattice sites of the N-SWCNTs. A high oxidation temperature of 785°C at which the rate of weight loss reaches the maximum value was demonstrated for the N-SWCNTs, indicative of their high-quality and good crystallinity. Furthermore, these

N-SWCNTs showed metallic behavior, as indicated by the low current on/off ratios of fabricated TFTs. Desirable ORR performance was demonstrated for the N-SWCNTs due to their C-N active sites and good conductivity.

Received 13 July 2015; accepted 2 August 2015; published online 19 August 2015

1 Dresselhaus MS, Dresselhaus G, Eklund P. Science of Fullerenes and Carbon Nanotubes. Waltham: Academic Press, 1996
2 Saito R, Dresselhaus G, Dresselhaus MS. Physical Properties of Carbon Nanotubes. London: Imperial College Press, 1998
3 Avouris P, Chen ZH, Perebeinos V. Carbon-based electronics. Nat Nanotechnol, 2007, 2: 605–615
4 Itkis ME, Yu A, Haddon RC. Single-walled carbon nanotube thin film emitter-detector integrated optoelectronic device. Nano Lett, 2008, 8: 2224–2228
5 Ding L, Wang S, Zhang ZY, *et al*. Y-contacted high-performance n-type single-walled carbon nanotube field-effect transistors: scaling and comparison with Sc-contacted devices. Nano Lett, 2009, 9: 4209–4214
6 Gabor NM, Zhong ZH, Bosnick K, *et al*. Extremely efficient multiple electron-hole pair generation in carbon nanotube photodiodes. Science, 2009, 325: 1367–1371
7 Mueller T, Kinoshita M, Steiner M, *et al*. Efficient narrow-band light emission from a single carbon nanotube p–n diode. Nat Nanotechnol, 2010, 5: 27–31
8 Tahvili MS, Jahanmiri S, Sheikhi MH. High-frequency transmission through metallic single-walled carbon nanotube interconnects. Int J Numer Modell Electron, 2009, 22: 369–378
9 Chai Y, Xiao Z, Chan PCH. Horizontally aligned carbon nanotube bundles for interconnect application: diameter-dependent contact resistance and mean free path. Nanotechnology, 2010, 21: 235705
10 Li H, Xu CA, Banerjee K. Carbon nanomaterials: the ideal interconnect technology for next-generation ICs. IEEE Des Test Comput, 2010, 27: 20–31
11 Yu B, Liu C, Hou PX, *et al*. Bulk synthesis of large diameter semiconducting single-walled carbon nanotubes by oxygen-assisted floating catalyst chemical vapor deposition. J Am Chem Soc, 2011, 133: 5232–5235
12 Ding L, Tselev A, Wang JY, *et al*. Selective growth of well-aligned semiconducting single-walled carbon nanotubes. Nano Lett, 2009, 9: 800–805
13 Hong G, Zhang B, Peng BH, *et al*. Direct growth of semiconducting single-walled carbon nanotube array. J Am Chem Soc, 2009, 131: 14642–14643
14 Harutyunyan AR, Chen GG, Paronyan TM, *et al*. Preferential growth of single-walled carbon nanotubes with metallic conductivity. Science, 2009, 326: 116–120
15 Hou PX, Li WS, Zhao SY, *et al*. Preparation of metallic single-wall carbon nanotubes by selective etching. ACS Nano, 2014, 8: 7156–7162
16 Wang Y, Liu YQ, Li XL, *et al*. Direct enrichment of metallic single-walled carbon nanotubes induced by the different molecular composition of monohydroxy alcohol homologues. Small, 2007, 3: 1486–1490
17 Sundaram RM, Koziol KKK, Windle AH. Continuous direct spinning of fibers of single-walled carbon nanotubes with metallic chirality. Adv Mater, 2011, 23: 5064–5068
18 Voggu R, Ghosh S, Govindaraj A, *et al*. New strategies for the enrichment of metallic single-walled carbon nanotubes. J Nanosci Nanotechnol, 2010, 10: 4102–4108
19 Hwang SK, Lee JM, Kim S, *et al*. Flexible multilevel resistive memory with controlled charge trap band N-doped carbon nanotubes. Nano Lett, 2012, 12: 2217–2221
20 Hashim DP, Narayanan NT, Romo-Herrera JM, *et al*. Covalently bonded three-dimensional carbon nanotube solids via boron induced nanojunctions. Sci Rep, 2012, 2: 363
21 Sumpter BG, Meunier V, Romo-Herrera JM, *et al*. Nitrogen-mediated carbon nanotube growth: diameter reduction, metallicity, bundle dispersability, and bamboo-like structure formation. ACS Nano, 2007, 1: 369–375
22 Gong KP, Du F, Xia ZH, *et al*. Nitrogen-doped carbon nanotube arrays with high electrocatalytic activity for oxygen reduction. Science, 2009, 323: 760–764
23 Maciel IO, Campos-Delgado J, Cruz-Silva E, *et al*. Synthesis, electronic structure, and Raman scattering of phosphorus-doped single-wall carbon nanotubes. Nano Lett, 2009, 9: 2267–2272
24 Campos-Delgado J, Maciel IO, Cullen DA, *et al*. Chemical vapor deposition synthesis of N-, P-, and Si-doped single-walled carbon nanotubes. ACS Nano, 2010, 4: 1696–1702
25 Fagan SB, Mota R, Silva AJR, *et al*. Substitutional Si doping in deformed carbon nanotubes. Nano Lett, 2004, 4: 975–977
26 Cruz-Silva E, López-Urías F, Muñoz-Sandoval E, *et al*. Electronic transport and mechanical properties of phosphorus- and phosphorus-nitrogen-doped carbon nanotubes. ACS Nano, 2009, 3: 1913–1921
27 Pattinson SW, Ranganathan V, Murakami HK, *et al*. Nitrogen-induced catalyst restructuring for epitaxial growth of multiwalled carbon nanotubes. ACS Nano, 2012, 6: 7723–7730
28 Barzegar HR, Gracia-Espino E, Sharifi T, *et al*. Nitrogen doping mechanism in small diameter single-walled carbon nanotubes: impact on electronic properties and growth selectivity. J Phys Chem C, 2013, 117: 25805–25816
29 Koós AA, Dowling M, Jurkschat K, *et al*. Effect of the experimental parameters on the structure of nitrogen-doped carbon nanotubes produced by aerosol chemical vapour deposition. Carbon, 2009, 47: 30–37
30 Pattinson SW, Diaz RE, Stelmashenko NA, *et al*. *In situ* observation of the effect of nitrogen on carbon nanotube synthesis. Chem Mater, 2013, 25: 2921–2923
31 Liu J, Rinzler AG, Dai HJ, *et al*. Fullerene pipes. Science, 1998, 280: 1253–1256
32 Maiti UN, Lee WJ, Lee JM, *et al*. 25th anniversary article: chemically modified/doped carbon nanotubes & graphene for optimized nanostructures & nanodevices. Adv Mater, 2014, 26: 40–67
33 Pint CL, Sun ZZ, Moghazy S, *et al*. Supergrowth of nitrogen-doped single-walled carbon nanotube arrays: active species, dopant characterization, and doped/undoped heterojunctions. ACS Nano, 2011, 5: 6925–6934
34 Yu B, Hou PX, Li F, *et al*. Selective removal of metallic single-walled carbon nanotubes by combined *in situ* and post-synthesis oxidation. Carbon, 2010, 48: 2941–2947
35 Hiraoka T, Izadi-Najafabadi A, Yamada T, *et al*. Compact and light supercapacitor electrodes from a surface-only solid by opened carbon nanotubes with 2200 m^2 g^{-1} surface area. Adv Funct Mater, 2010. 20: 422–428
36 Zhu J, Wang Y, Li WJ, *et al*. A density functional study of nitrogen adsorption in single-wall carbon nanotubes. Nanotechnology, 2007, 1: 095707
37 Zhang XR, Wang WC, Chen JF, Shen ZG. Characterization of a sample of single-walled carbon nanotube array by nitrogen adsorption isotherm and density functional theory. Langmuir, 2003, 19: 6088–6096
38 Beguin F, Frackowiek E (eds.). Carbons for Electrochemical Energy

Storage and Conversion Systems. Boca Raton: CRC Press, 2010
39 Villalpando-Paez F, Zamudio A, Elias AL, *et al.* Synthesis and characterization of long strands of nitrogen-doped single-walled carbon nanotubes. Chem Phys Lett, 2006, 424: 345–352
40 Zhou W, Ooi YH, Russo R, *et al.* Structural characterization and diameter-dependent oxidative stability of single wall carbon nanotubes synthesized by the catalytic decomposition of CO. Chem Phys Lett, 2001, 350: 6–14
41 Liu Y, Jin Z, Wang JY, *et al.* Nitrogen-doped single-walled carbon nanotubes grown on substrates: evidence for framework doping and their enhanced properties. Adv Funct Mater, 2011, 21: 986–992
42 Maciel IO, Anderson N, Pimenta MA, *et al.* Electron and phonon renormalization near charged defects in carbon nanotubes. Nat Mater, 2008, 7: 878–883
43 Maciel IO, Pimenta MA, Terrones M, *et al.* The two peaks G' band in carbon nanotubes. Phys Status Solidi B, 2008, 245: 2197–2200
44 Hou PX, Orikasa H, Yamazaki T, *et al.* Synthesis of nitrogen-containing microporous carbon with a highly ordered structure and effect of nitrogen doping on H_2O adsorption. Chem Mater, 2005, 17: 5187–5193

Acknowledgement This work was financially supported by the National Basic Research Program of China (2011CB932601), National Natural Science Foundation of China (51221264, 51272257, and 51372254), and Chinese Academy of Sciences (KGZD-EW-T06).

Author contributions Hou PX, Liu C, and Cheng HM designed the project and the experiments. Song M, Li JC, and Li SS performed the experiments. Hou PX and Song M analysed the results and wrote the paper.

Conflict of interest The authors declare that they have no conflict of interest.

Supplementary information Supporting data are available in the online version of the paper.

Peng-Xiang Hou is a professor in materials science and engineering at the Institute of Metal Research, Chinese Academy of Sciences (CAS). She received her BSc and PhD degrees, both in materials science from the Institute of Metal Research in 1999 and 2003, respectively. Her research focuses on the controlled synthesis, properties and applications of single-wall carbon nanotubes.

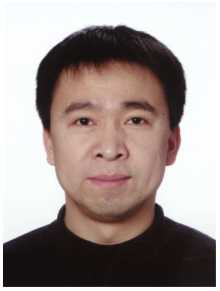

Chang Liu is a professor at the Institute of Metal Research, CAS. He received his PhD degree in materials science in 2000 at the Institute of Metal Research, CAS. He is a group leader of "Synthesis, Property and Application of Carbon Nanotubes".

中文摘要 本文以二茂铁为催化剂、三聚氰胺为氮源、甲烷为碳源, 采用浮动催化剂化学气相沉积法制备了氮掺杂单壁碳纳米管. 通过控制三聚氰胺的挥发量, 实现了氮原子在单壁碳纳米管石墨网格中的微量掺杂, 获得了高质量的氮掺杂单壁碳纳米管, 其抗氧化温度高达795°C. 这种微量氮掺杂使得单壁碳纳米管的直径变小、直径分布范围变窄, 并表现出金属性行为及提高的氧还原性能.